Partial Deletion of Glycoprotein B5R Enhances Vaccinia Virus Neutralization Escape while Preserving Oncolytic Function

Motomu Nakatake,[1] Hajime Kurosaki,[1] Nozomi Kuwano,[1] Kosuke Horita,[1] Mai Ito,[1] Hiromichi Kono,[1] Tomotaka Okamura,[2] Kosei Hasegawa,[3] Yasuhiro Yasutomi,[2] and Takafumi Nakamura[1]

[1]Division of Molecular Medicine, Department of Biomedical Science, Graduate School of Medical Sciences, Tottori University, 86 Nishi-cho, Yonago 683-8503, Japan; [2]Laboratory of Immunoregulation and Vaccine Research, Tsukuba Primate Research Center, National Institutes of Biomedical Innovation, Health and Nutrition, Tsukuba, Ibaraki 305-0843, Japan; [3]Department of Gynecologic Oncology, Saitama Medical University International Medical Center, 1397-1, Yamane, Hidaka-City, Saitama 350-1298, Japan

Vaccinia virus (VV) has been utilized in oncolytic virotherapy, but it risks a host antiviral immune response. VV has an extracellular enveloped virus (EEV) form consisting of a normal virion covered with a host-derived outer membrane that enables its spread via circulation while evading host immune mechanisms. However, the immune resistance of EEV is only partial, owing to expression of the surface protein B5R, which has four short consensus repeat (SCR) domains that are targeted by host immune factors. To engineer a more effective virus for oncolytic virotherapy, we developed an enhanced immune-evading oncolytic VV by removing the SCRs from the attenuated strain LC16mO. Although deletion of only the SCRs preserved viral replication, progeny production, and oncolytic activity, deletion of whole B5R led to attenuation of the virus. Importantly, SCR-deleted EEV had higher neutralization resistance than did B5R-wild-type EEV against VV-immunized animal serum; moreover, it retained oncolytic function, thereby prolonging the survival of tumor-bearing mice treated with anti-VV antibody. These results demonstrate that partial SCR deletion increases neutralization escape without affecting the oncolytic potency of VV, making it useful for the treatment of tumors under the anti-virus antibody existence.

INTRODUCTION

Oncolytic virotherapy is a novel anti-cancer strategy that has shown promising clinical results in the U.S. Food and Drug Administration-approved talimogene laherparepvec. Several viruses have been engineered as next-generation oncolytic agents with their functionalities enhanced via viral recombination,[1–3] loading of therapeutic factors,[4] or combination with conventional therapies.[4,5] However, oncolytic viruses elicit antiviral immune responses in the host that significantly limit their therapeutic potential, especially in reaching remote tumors.[6–8]

Vaccinia virus (VV) can escape antiviral immunity using a unique infectious form—namely, the extracellular enveloped virus (EEV).[9]

Most progeny virions mature as the normal infectious form, intracellular mature virus (IMV), and are released after host cell death; however, a few are covered with or wrapped in early endosomes or a *trans*-Golgi network, yielding an intracellular enveloped virus (IEV) that is exposed on the cell surface (referred to as a cell-associated virus) via membrane fusion before being released as an EEV through actin polymerization.[9] EEVs are far less abundant than IMVs, representing <1% of total infectious virions;[10] however, they have advantages in viral dissemination, such as rapid spreading without causing host cell death[9,11] and efficient entry into target cells independent of cell-signaling mechanisms.[12,13] In addition, the EEV outer membrane presents host-derived antigens, such as complement control proteins (e.g., cluster of differentiation [CD]46, CD55, and CD59) and major histocompatibility complex class I,[14,15] which allow the virus to spread systemically via circulation while escaping neutralization by complement factors or anti-VV antibodies.[15,16]
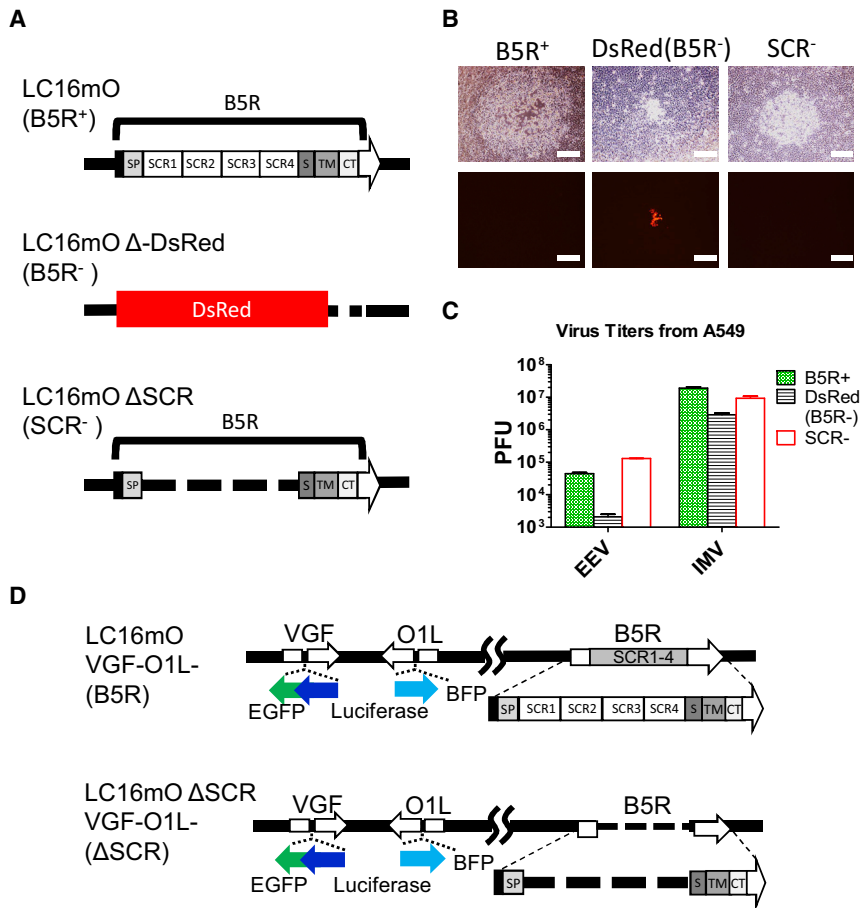
Some engineered VV strains produce large amounts of EEV (e.g., International Health Department (IHD)-J, vA34R, or WI) due to a point mutation in glycoprotein A34R,[17] making them suitable for oncolytic virotherapy.[2,3] However, EEV has only partial immune resistance, although it is higher than that of IMV. Of the five EEV outer membrane surface antigens (A33R, A34R, A36R, A56R, and B5R), B5R is the most frequent target of host-neutralizing antibodies.[18,19] B5R is a 42-kDa envelope glycoprotein containing four short consensus repeat (SCR) domains, whose expression is critical for viral morphogenesis, trafficking, dissemination, and EEV production.[20–25] However, anti-B5R antibody recognizing the SCR1/SCR2 boundary and/or the B5R stalk region[26] induces complement-dependent EEV neutralization.[27–29]

A

LC16mO
(B5R⁺)

LC16mO Δ-DsRed
(B5R⁻)

LC16mO ΔSCR
(SCR⁻)

B

B5R⁺   DsRed(B5R⁻)   SCR⁻

C

D

LC16mO
VGF-O1L-
(B5R)

LC16mO ΔSCR
VGF-O1L-
(ΔSCR)

Figure 1. Phenotypic Differences among B5R Recombinant Viruses

(A) Schematic representation of the B5R recombinant VVs LC16mO (B5R⁺), LC16mO Δ-DsRed (B5R⁻), and LC16mO ΔSCR (SCR⁻). (B) RK13 cells were infected with the three B5R recombinant viruses, and viral plaques were photographed 48 h later. Top shows phase-contrast images, and bottom shows fluorescence micrographs of the same fields. Scale bar, 500 μm. (C) EEV and IMV were recovered from culture supernatants or lysates of A549 lung carcinoma cells infected with the three B5R recombinant viruses at an MOI of 0.1, and they were individually titrated in RK13 cells. Total PFU was calculated from plaque numbers and total volume of viral reagent. Data represent mean ± SD (n = 3). (D) Schematic representation of the VGF- and O1-deleted virus B5R LC16mO VGF⁻/O1⁻ (B5R) and SCR-deleted virus LC16mO ΔSCR VGF⁻/O1⁻ (ΔSCR).

Whole B5R deletion drastically reduces viral plaque size, pathogenicity, actin polymerization, and EEV production.[21,24,25,30] In contrast, partial SCR deletion causes a variety of viral phenotypes, including a mild reduction in plaque size[22] and comet-shaped spreading similar to that seen in IHD-J.[18,22,23,31] Interestingly, SCR deletion reportedly increases EEV production in rabbit kidney RK13 cells,[22,23] despite the loss of actin polymerization.[22–24,31] Since SCR domains are responsible for EEV neutralization, their deletion may allow the virus to evade anti-B5R antibody[18] without affecting its capacity for replication or oncolytic activity.

To examine the above possibility, we reinforced an immune-evasive form of oncolytic VV by partially deleting the SCRs. This ΔSCR virus was structured from the low-neurovirulent LC16mO strain isolated from the Lister strain through repeated passaging and selection for temperature sensitivity.[32,33] Tumor specificity was conferred by limiting viral replication in normal cells via deletion of the two viral mitogen-activated protein kinase-dependent growth factors VV growth factor (VGF) and O1.[34] The resultant ΔSCR EEV showed enhanced resistance to anti-VV-neutralizing serum and antibody (Ab) compared to that of VV with intact B5R, while replication, progeny virus production, and oncolytic potency were unaffected. Our re-

sults demonstrate that ΔSCR can be an effective agent for cancer treatment, including in patients with pre-existing neutralizing antibodies.

RESULTS

B5R Deletion Affects Vaccinia Viral Phenotype

The effects of B5R mutation were evaluated using three recombinant VVs, namely, B5R-wild-type (WT) LC16mO, B5R-deleted LC16mO Δ-DsRed, and SCR-deleted LC16mO ΔSCR (Figure 1A). B5R deletion affected not only viral pathogenicity but also phenotype, including plaque formation and progeny virus production. The reduction in viral plaque size was proportional to the extent of B5R deletion, with LC16mO ΔSCR generating plaques of an intermediate size between the normal-sized LC16mO plaques and smaller LC16mO Δ-DsRed plaques (Figure 1B). Progeny virus production was markedly reduced by complete deletion of B5R, but not SCR. LC16mO Δ-DsRed showed decreased EEV and IMV production compared to that of LC16mO (Figure 1C); in contrast, progeny virus production was mostly unaltered for LC16mO ΔSCR, but EEV production in A549 lung carcinoma cells was increased.

SCR Deletion Alters EEV Generation without Reducing Normal Progeny Virus Production and Oncolytic Activity

Progeny virus production by B5R-WT and SCR-deleted viruses was evaluated in various human cancer cell lines. VGF and O1 were deleted in both viruses to confer tumor-specific viral replication (Figure 1D), yielding B5R-WT LC16mO VGF⁻/O1⁻ and SCR-deleted LC16mO ΔSCR VGF⁻/O1⁻, which are hereafter referred to as B5R and ΔSCR, respectively. Deletions were achieved by inserting a gene cassette, harboring the firefly luciferase gene fused to EGFP- or blue fluorescent protein (BFP)-encoding genes, into each locus. B5R gene expression was confirmed from those VGF⁻/O1⁻ viruses by RT-PCR (Figure S1A).

Table 1. Ratio of B5R and ΔSCR Progeny Virus Production

Tumor Cell Line		EEV Ratio (ΔSCR:B5R)	IMV Ratio (ΔSCR:B5R)
Type	Name		
Ovarian	A2780	6.333**	1.523
	CaOV3	7.159***	1.657*
	RMG-1	1.825**	0.75
	SKOV3	1.835*	1.161
Pancreatic	AsPC1	0.969	0.837
	BxPC3	0.091***	0.551
	Panc1	0.418**	0.249**
	SW1990	0.952	0.636
Colon	Caco2	0.992	0.968
	HT29	0.229**	0.279**
	LoVo	2.719*	0.654
	SW480	0.254*	0.961
Lung	A549	4.634***	0.425**
Breast	MCF-7	0.913	1.217
	SK-BR-3	1.223	0.664
Hepatocellular	HepG2	3.164**	1.242
Neuroblastoma	SK-N-AS	0.766	0.621
	SK-N-BE	0.335	0.676
Epidermoid	A431	1.132	1.198
	Hep2	0.436*	1.267

Various tumor cell lines were infected with B5R or ΔSCR at an MOI of 0.1. EEVs and IMVs were recovered from the cultures 48 h later, and they were titrated in RK13 cells as described in Figure 1C. The table shows the progeny virus productive ratio of ΔSCR to B5R. Titers are listed in Figure S2. *p < 0.05, **p < 0.01, ***p < 0.001 (unpaired t test).

EEV and IMV were recovered from various human cancer cell lines infected with B5R or ΔSCR at an MOI of 0.1, and they were titrated in RK13 cells. EEV or IMV phenotype was distinguished concisely by detecting host cellular CD46 and viral D8L. Both EEV and IMV expressed the viral D8L protein, but host cellular CD46 was presented only in EEV covered with host-derived membrane (Figure S1B). EEV production by B5R and ΔSCR viruses differed in the various human cancer cell lines (Table 1; Figure S2); ΔSCR increased EEV production in all ovarian carcinoma cell lines (A2780, CaOV3, RMG-1, and SKOV3), LoVo colon carcinoma cells, HepG2 hepatocellular carcinoma cells, and A549 cells, but it decreased production in BxPC3 and Panc1 pancreatic cancer cells, HT29 and SW480 colon carcinoma cells, and Hep2 laryngeal carcinoma cells (all p < 0.05). On the other hand, most cell lines showed no differences between IMV production by B5R and ΔSCR viruses, with only four cell lines showing statistically significant differences.

The oncolytic activity of B5R and ΔSCR was compared in human ovarian cancer cell lines, which tend to have high EEV production. Cells were separately infected with EEV from culture supernatant or with whole virus including IMV, and cell viability was evaluated. Viral infection area increased in A2780 and CaOV3 cells upon infec-tion with ΔSCR-derived EEV (Figure 2A), with a concomitant decrease in viability as compared to cells treated with B5R-derived EEV (Figure 2B). There were no differences in infection area or viability between RMG-1 and SKOV3 ovarian carcinoma cells (Figures 2A and 2B). On the other hand, viral expansion and viability were comparable between B5R and ΔSCR following whole-virus infection (Figures 2C and 2D). These results are consistent with the observed IMV productivity of each virus (Table 1; Figure S2B).
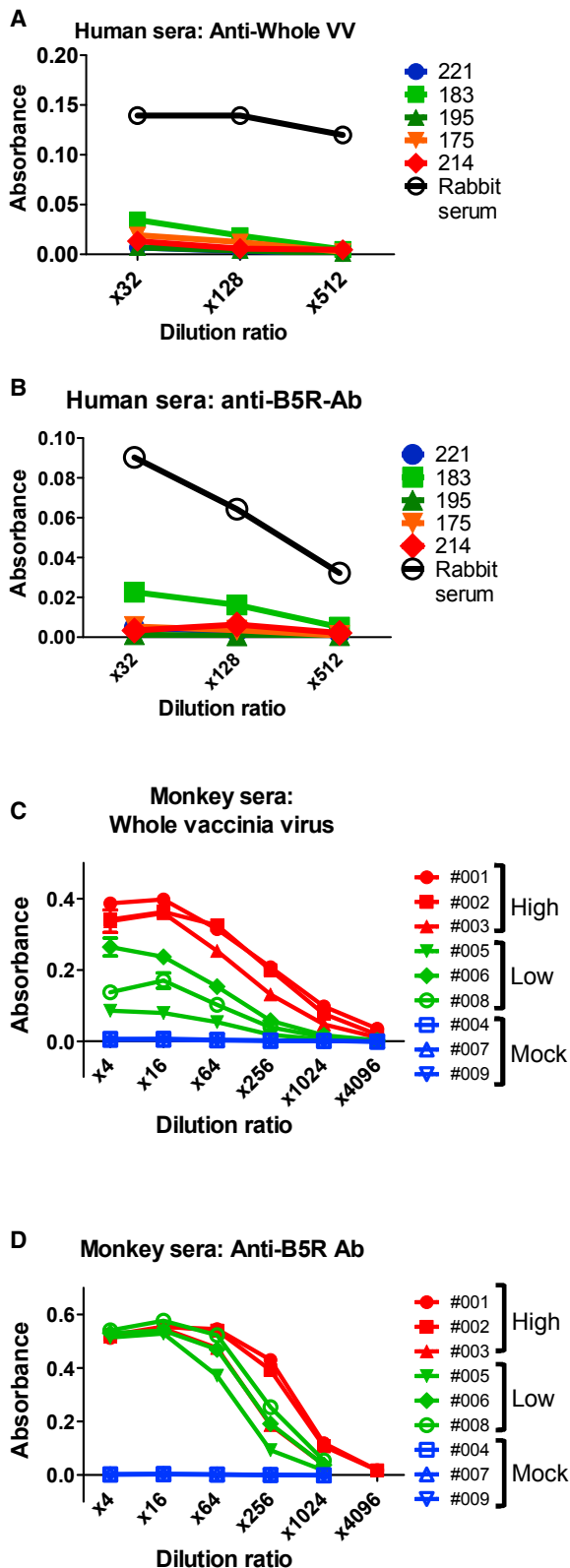
SCR-Deleted EEV Escapes Neutralization by Immunized Serum

Next, to compare the neutralization resistance of EEVs derived from B5R and ΔSCR, we explored anti-B5R Ab (an EEV-neutralizing Ab) from human serum samples. Derived from patients who received smallpox vaccinations, 20 human serum samples were used to calculate 50% neutralization doses (ND_{50}) against vaccinia virus (Table S1). Five of 20 samples showed neutralizing activity, but titers were undetectable in the other 15. The 5 serum samples, 221 (ND_{50}: not detected), 183, 195, 175, and 214 (ND_{50}: 16.09, 50.26, 53.55, and 114.77, respectively), were chosen for detecting the Ab response against whole VV and B5R by ELISA.

The results showed almost no anti-VV and anti-B5R antibodies even in the sample with the highest ND_{50}, 214 (Figures 3A and 3B). This suggests that most patients have no pre-existing antibodies against VV (including its EEV form). Therefore, artificially immunized animal serum was used to explore anti-EEV Abs. The ND_{50} and ELISA titer were measured in serum derived from cynomolgus monkeys treated with three different doses of VV (high dose = 10^8 plaque-forming units [PFU], low dose = 10^7 PFU, and mock = 0 PFU) (Table S2; Figures 3C and 3D). In immunized serum (non-mock treated), neutralization activity and antibody response against whole VV and B5R increased as a function of viral dose (Table S2; Figures 3C and 3D). Thus, the serum had potential for EEV neutralization.

To compare neutralization resistance, monkey serum samples were mixed with progeny virions from B5R or ΔSCR, and GFP expression and cytotoxicity of the escaped viruses were evaluated. Half or nearly all B5R EEV was neutralized by 1% high (001) or low (006) VV dose-immunized serum. In contrast, ΔSCR EEV escaped neutralization at the same concentration of immunized serum (Figure 4A). Quantification of GFP fluorescence revealed that ΔSCR EEV had higher replicative capacity than did B5R EEV, especially when mixed with 0.5% or 1% immunized serum (Figure 4B). Furthermore, cell viability was inversely proportional to viral GFP expression, and it was lower for ΔSCR EEV mixed with 0.5% or 1% high or low VV dose-immunized serum than for B5R EEV (Figure 4C). In IMV neutralization, B5R and ΔSCR were inhibited by almost comparable concentrations of immunized serum (Figure 4D). These findings are consistent with observed trends for viral replication and oncolytic activity; that is, B5R and ΔSCR IMVs showed similar variations in GFP expression (Figure 4E) and infected cell viability (Figure 4F). Thus, SCR deletion affects EEV, but not IMV, and ΔSCR-derived

A

B

C

D

was observed by fluorescence microscopy. B5R EEV showed slight resistance to anti-virus antibody and complement alone, but it was strongly suppressed by the combination of >0.2% antibody and 3% complement (Figure 5A). ΔSCR EEV showed higher immune resistance than did B5R EEV, escaping mixtures of up to 0.5% antibody and 10% complement. Accordingly, ΔSCR EEV showed higher GFP than B5R expression when mixed with antibody and complement (Figure 5B). Similar results were obtained using RMG-1 (Figure S3A) and A2780 (data not shown) cells as EEV-producing and -infecting cells, respectively. ΔSCR EEV decreased the viability of RMG-1 cells more than did B5R EEV when mixed with antibody and 3%–10% complement (Figure S3B).

Neither IMV escaped anti-virus antibody and complement alone or in combination (Figure 5C). Both B5R and ΔSCR IMVs were strongly inhibited by >0.2% antibody and/or 3% complement. There was no difference in viral GFP expression between B5R and ΔSCR IMVs (Figure 5D). These results suggest that EEV neutralization depends on the combination of antibody and complement, and SCR-deleted VV efficiently escapes their neutralizing activity.

EEV has higher neutralization resistance than does B5R EEV against whole serum derived from immunized monkeys.

SCR-Deleted VV Escapes Complement-Dependent EEV Neutralization

EEV is neutralized by anti-B5R antibody combined with complement;[27–29] we therefore mixed EEV and IMV derived from B5R and ΔSCR with rabbit anti-VV antibody (immunoglobulin G [IgG] fraction, anti-B5R antibody was detected by ELISA; data not shown) and rabbit complement separately. These mixtures were used to infect SKOV3 cells, and the replication of active virus

SCR Deletion Enhances the Oncolytic Activity of EEV in the Presence of Anti-virus Antibody

The neutralization resistance and oncolytic activity of EEVs were examined in a mouse model of anti-VV antibody-induced peritoneal dissemination. Athymic nude mice bearing A2780 ovarian cancer cells were injected with anti-VV antibody (IgG fraction) derived

A

Human sera: Anti-Whole VV

Legend:
- 221
- 183
- 195
- 175
- 214
- Rabbit serum

B

Human sera: anti-B5R-Ab

Legend:
- 221
- 183
- 195
- 175
- 214
- Rabbit serum

C

Monkey sera: Whole vaccinia virus

Legend:
- #001 — High
- #002 — High
- #003 — High
- #005 — Low
- #006 — Low
- #008 — Low
- #004 — Mock
- #007 — Mock
- #009 — Mock

D

Monkey sera: Anti-B5R Ab

Legend:
- #001 — High
- #002 — High
- #003 — High
- #005 — Low
- #006 — Low
- #008 — Low
- #004 — Mock
- #007 — Mock
- #009 — Mock

Figure 3. Detection of Anti-VV and -B5R Antibody in Serum

(A) Whole-VV antigen-coated wells were incubated with 4-fold serial dilutions (×32, ×128, ×512) of 5 human sera (patients 221, 183, 195, 175, and 214) or control immunized rabbit IgG. Antibody response was detected by measuring optical density at 405 nm (OD_{405}) after incubation with horseradish peroxidase-conjugated rabbit anti-human IgG (SouthernBiotech) and substrate. (B) Purified B5R protein-coated wells were incubated with the same serial dilutions of human serum and secondary antibody shown in (A), and antibody response was detected as described above. (C) Whole-VV antigen-coated wells were incubated with 4-fold serial dilutions (×4–4,096) of serum from monkeys immunized with high (001, 002, and 003) or low (005, 006, and 008) doses of VV or from mock-immunized monkeys (004, 007, and 009). Antibody response was detected after incubation with horseradish peroxidase-conjugated goat anti-monkey IgG (Abcam) and substrate. (D) Purified B5R protein-coated wells were incubated with the same serial dilutions of monkey serum shown in (C), and antibody response was detected as described above. Data in (A)–(D) are presented as means ± SD (n = 2).

from immunized rabbit or PBS, followed by intraperitoneal injection of B5R or ΔSCR EEV. Viral replication and tumor growth were evaluated based on firefly luciferase (Fluc) and *Renilla* luciferase (Rluc) expression, respectively.

Fluc luminescence reflecting viral distribution was reduced by antibody pretreatment on day 3 after virus injection; however, on day 7, ΔSCR EEV showed higher replication than did B5R EEV in the presence of antibody (Figure 6A, middle). On the other hand, the level of Rluc luminescence in tumors, which reflected tumor growth, was similar among mice before virus injection (Figure 6A, top), but it disappeared on day 8 after injection upon the administration of either B5R or ΔSCR EEV without antibody pretreatment. In contrast, in the presence of antibody, tumors disappeared in half of ΔSCR EEV-treated mice, while they only disappeared in a single B5R EEV-treated mouse (Figure 6A, bottom).

Quantitative analysis of viral Fluc luminescence revealed that the replication kinetics of both EEVs were similar in the absence of antibody (Figure 6B). When antibody was present, the peak intensity of viral Fluc signals was delayed 2 days by ΔSCR EEV and 5 days by B5R EEV (Figure 6B). ΔSCR EEV showed higher replication than did B5R EEV on day 7 after virus injection with antibody pretreatment (p < 0.05). Quantification of tumor Rluc luminescence indicated that the signal in mice without antibody treatment was almost completely abolished by B5R and ΔSCR EEVs. In contrast, ΔSCR EEV suppressed tumor signals in antibody-treated mice to levels in mice without antibody treatment, whereas the anti-cancer effect of B5R EEV was strongly inhibited by antibody treatment (Figure 6C). The survival of mice was prolonged by injection with B5R and ΔSCR EEVs without anti-VV antibody treatment as compared to survival after mock treatment (Figure 6D). Meanwhile, ΔSCR EEV prolonged the survival of mice with and without antibody treatment, although antibody treatment reduced survival in B5R EEV-treated mice (Figure 6D). The log rank test showed that the B5R EEV-antibody combination prolonged survival compared to that in mice treated with PBS-antibody (p = 0.0041); however, ΔSCR EEV-antibody had an even greater effect (p = 0.0291). Thus, B5R and ΔSCR EEVs have comparable therapeutic efficacies in the absence of
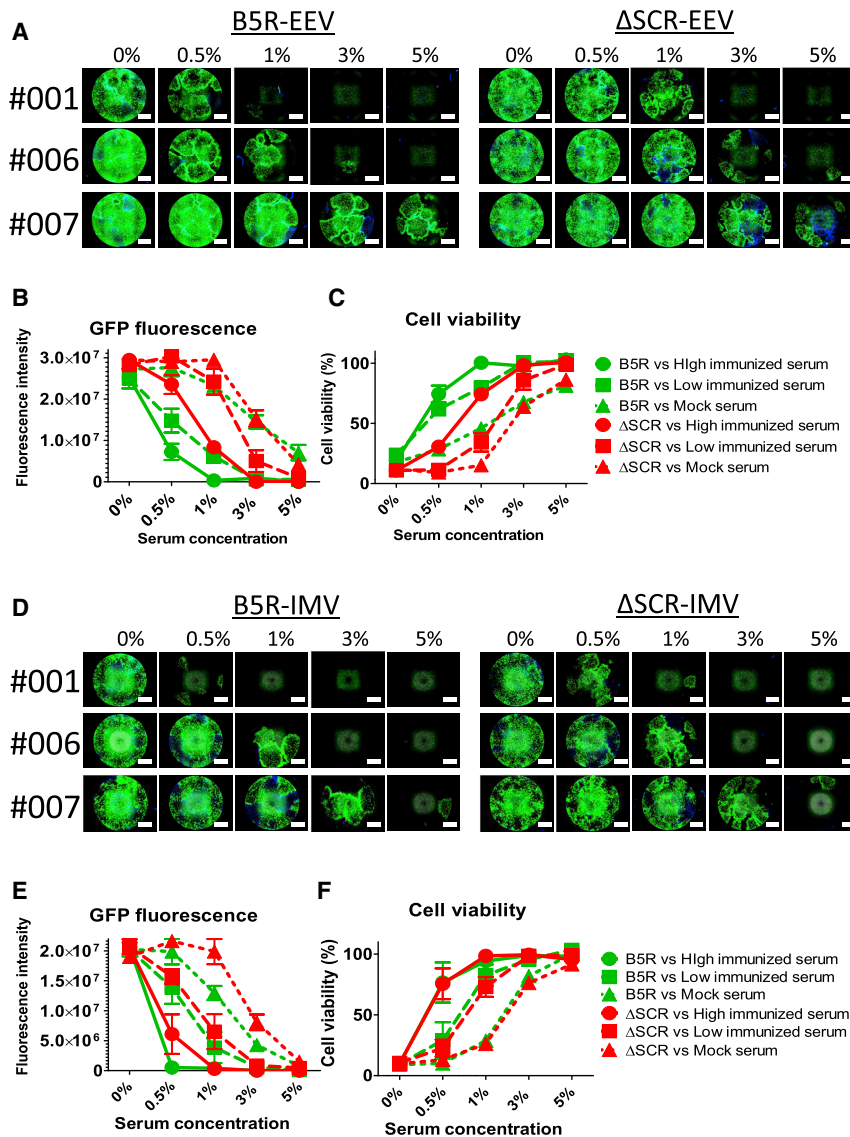
Figure 4. Neutralization Resistance of EEV or IMV against Immunized Monkey Serum

(A) EEV in the supernatant of RMG-1 cells infected with B5R or ΔSCR was mixed with 0%, 0.5%, 1%, 3%, and 5% serum from monkeys immunized with a high (001: 1×10^8 PFU by intravenous injection) or low (006: 1×10^7 PFU by intravenous injection) dose of VV or from a mock-immunized (007) monkey. The mixtures were used to infect RMG-1 cells, which were imaged by phase-contrast and fluorescence microscopy 120 h later. Scale bar, 1,500 μm. (B) Quantification of GFP fluorescence shown in (A). (C) Viability of infected cells described in (A) expressed as percent cell survival of mock-infected cells. B5R and ΔSCR EEVs differed in terms of cytolytic activity when mixed with 0.5% (high dose, p = 0.0042 and low dose, p = 0.0012; unpaired t test) or 1% (high dose, p = 0.0007 and low dose, p = 0.0044; unpaired t test) serum from immunized monkeys. (D) IMV in the lysate of RMG-1 cells infected with B5R or ΔSCR was used to infect RMG-1 cells as described (A). Images were acquired 120 h later. (E) Quantification of GFP fluorescence in (D). (F) Viability of cells in (D). Data in (B), (C), (E), and (F) are presented as means ± SD (n = 3).

potently inhibits viral delivery to remote organs,[3,6–8] virus injection is basically limited to the intratumoral route. Although various strategies have been developed to escape anti-viral immunity, such as carrier-cell therapy,[5,7] lipid coating,[37] and immunosuppression,[6–8,36] there are none based on viruses alone.

In this study, we enhanced the ability of an immune-resistant form of VV to escape host anti-virus antibody by partially deleting the antigenic SCR region of the viral glycoprotein B5R. Whole-B5R deletion significantly reduced viral plaque size as well as both EEV and IMV production (Figures 1B and 1C). SCR-deleted virus (ΔSCR) had an intermediate plaque size between those of whole-B5R deletion and WT viruses (Figure 1B), which is consistent with a previous report.[22] However, SCR deletion had almost no effect on IMV production (Figure 1C; Figure S2B) or oncolytic activity compared to levels after infection by the WT virus (B5R) (Figures 2C and 2D), and it tended to increase EEV production, especially in ovarian cancer cell lines such as A2780 and CaOV3 (Table 1; Figure S2A), which showed decreased viability with increasing EEV titer (Figure 2B). These symptoms suggest the potential of EEV utilization because of the lower productivity of the WT virus.

The effect of ΔSCR on EEV production varied among tumor cell types, suggesting the influence of host cell factors on EEV morphogenetic processes, such as viral entry, transport, wrapping, exposure, or egress. In contrast, IMV formation was unaffected, as

anti-virus antibody, whereas ΔSCR EEV is more potent when antibody is present.

DISCUSSION

The balance of antitumor and antiviral immunity is the most important determinant of the efficacy of oncolytic virotherapy; the efficacy is enhanced by the former and inhibited by the latter. Anti-tumor immunity can be enhanced by several strategies, including the loading of immunotherapeutic agents (e.g., cytokines, chemokines, and co-stimulation molecules) and/or combined immune-checkpoint blockade.[4] Pre-existing antiviral immunity does not necessarily inhibit the viral therapeutic effect, especially in the case of direct intratumoral injection.[35] However, there is evidence that the oncolytic effect of therapeutic viruses is enhanced by immunosuppression.[6,8,36] Furthermore, since pre-existing immunity
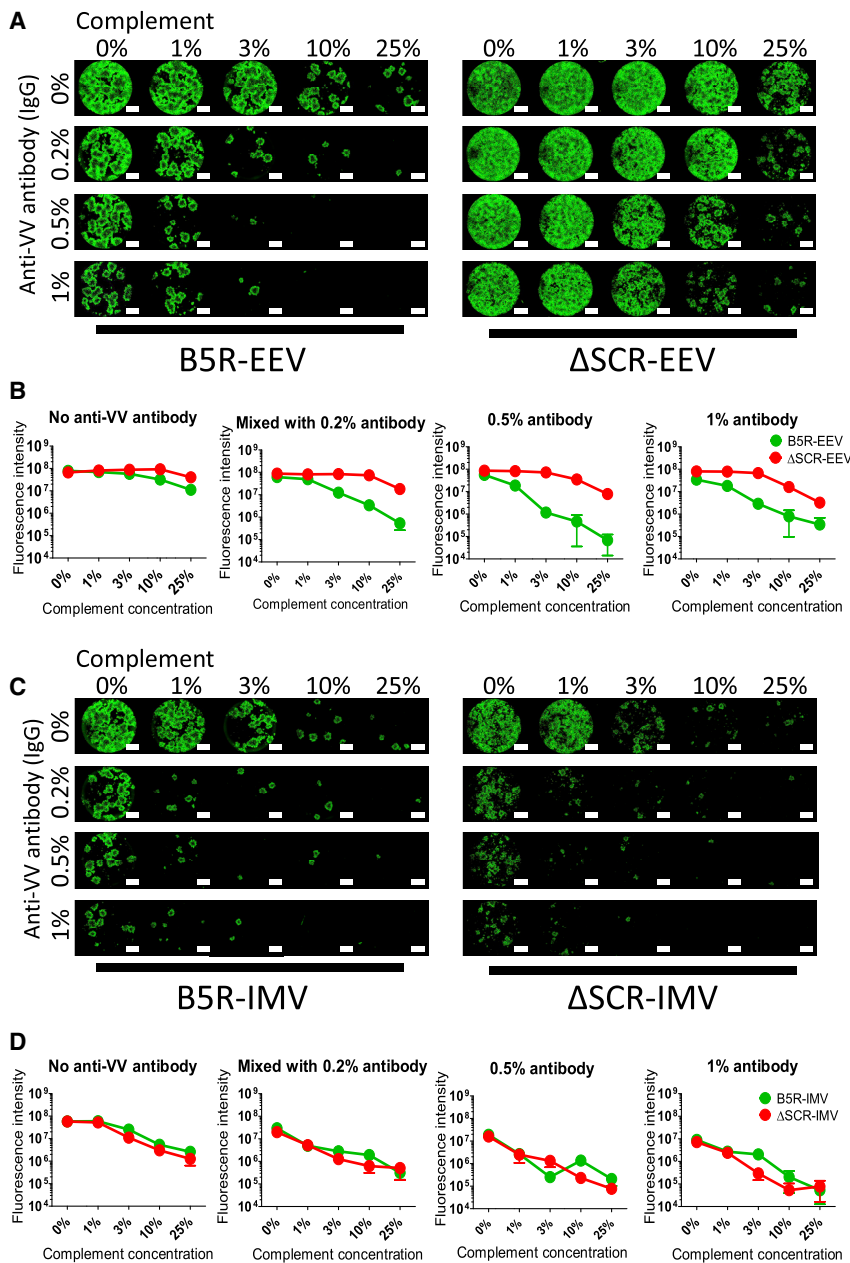
Figure 5. Neutralization Resistance of SCR-Deleted EEV or IMV against Anti-virus Antibody and Complement

(A) EEV in the culture supernatant of SKOV3 cells infected with B5R or ΔSCR was mixed with 0%, 0.2%, 0.5%, or 1% rabbit anti-VV-immunized serum (IgG fraction) and/or 0%, 1%, 3%, 10%, or 25% rabbit complement. The mixture was used to infect SKOV3 cells, which were photographed under a fluorescence microscope 96 h after infection. Scale bar, 1,500 μm. (B) Quantification of GFP fluorescence described in (A) as a function of serum (IgG) concentration. (C) IMV produced from lysates of SKOV3 cells infected with B5R or ΔSCR was mixed and used for SKOV3 cell infection as described (A). Images were acquired 96 h later. (D) Quantification of GFP fluorescence in (C). Data in (B) and (D) are presented as means ± SD (n = 3).

egress by detaching from the cell surface due to loss of interaction between the luminal domain of B5R and the plasma membrane, similar to SCR4-mutated (B5R^{P189S}) VV.[41] Thus, cells with high EEV productivity may support viral wrapping and/or transport out of the cell in the case of ΔSCR.

There are several factors that may facilitate the processes described above. For example, RAB1A—a member of the Ras oncogene family—mediates trafficking of matured virions to the wrapping site.[42] During the wrapping process, VV utilizes retrograde transport factors in the Golgi-associated transport pathway, such as syntaxin 6 and vacuolar protein sorting 52 homolog.[43,44] In addition, wrapped virions (IEV) employ microtubule transport to reach the cell membrane through recruitment of kinesin-1 by the IEV-associated protein A36R.[45–47] The kinesin-1 component KIF5B is associated with lung cancer prognosis,[48] and other kinesin family members have also been implicated in the progression of various malignancies, including ovarian cancer.[49–51] Microtubule dynamics are important not only to tumor growth but also to drug resistance, especially to those used to treat ovarian cancers, as these mainly target the tumor cell cytoskeleton.[52,53]

evidenced by the comparable levels of IMV productivity of B5R and ΔSCR. B5R regulates several aspects of morphogenesis; however, EEV entry requires an intact B5R stalk region,[38] while mature virion transfer and accumulation in the wrapping region depend on the transmembrane domain and cytoplasmic tail of B5R, respectively, but not on the SCRs.[39] A major function of the SCRs is to mediate switching from microtubule transport to actin-based motility during EEV exposure at the cell surface.[40] SCR4 is the region responsible for this activity, but the ΔSCR virus maintained or increased EEV productivity in various tumor cell lines (>70% of cells, as shown in Table 1). ΔSCR EEV may readily

As for preexisting anti-virus antibodies, we explored anti-VV and -B5R (EEV-specific) antibodies from human and immunized monkey serum. Interestingly, there were almost no VV- or B5R-specific antibodies in the vaccinated human serum (Figures 3A and 3B). This result is consistent with past clinical reports of systemic VV treatment, which resulted in comparable therapeutic effects regardless of base neutralizing titer or vaccination history.[54,55] This suggests that most patients have few pre-existing antibodies that neutralize the
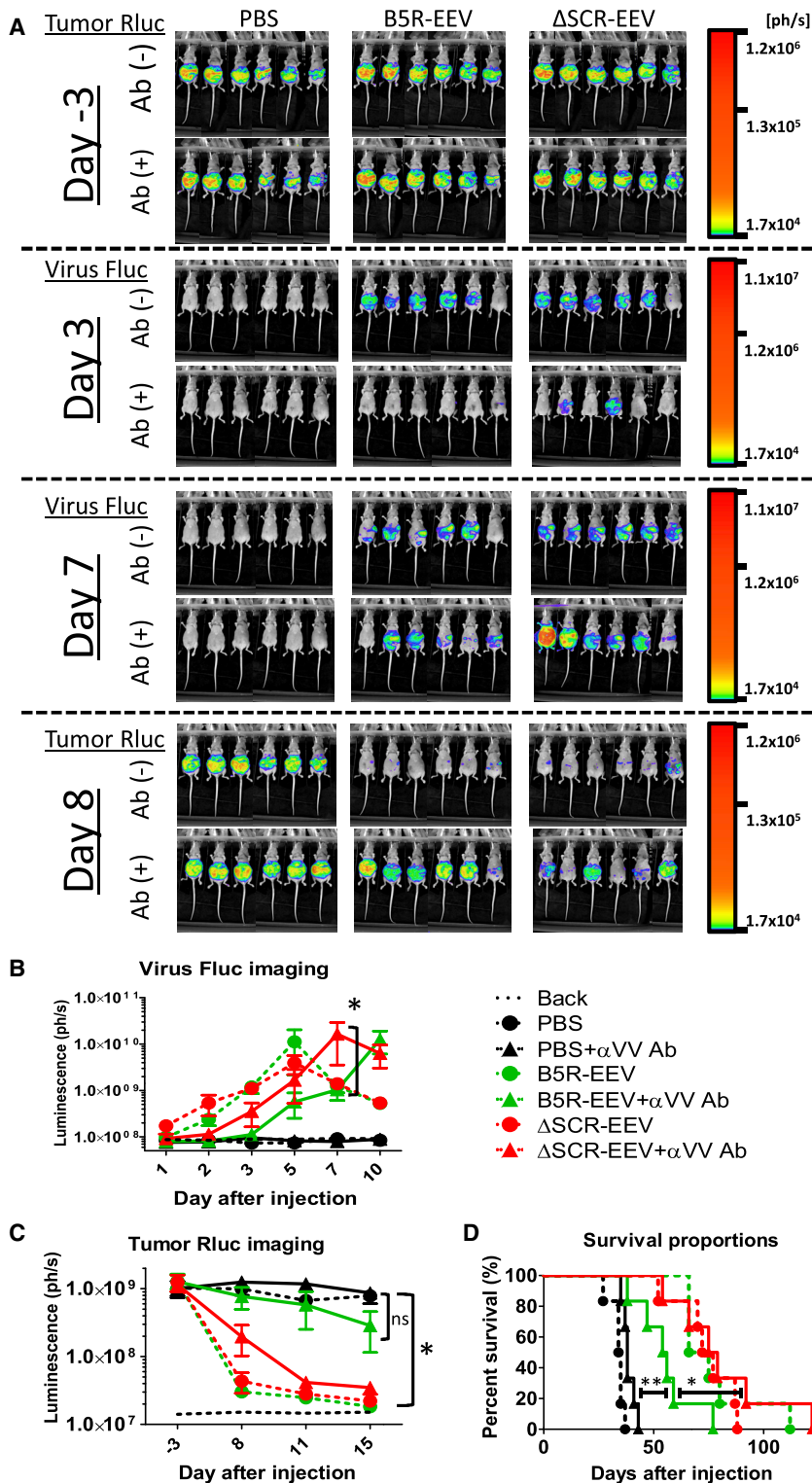
Figure 6. SCR-Deleted EEV Maintains Oncolytic Activity *In Vivo* in the Presence of Vaccinia-Neutralizing Antibodies

(A) *In vivo* bioluminescence imaging of tumor burden and viral replication. Athymic nude mice with peritoneal dissemination of A2780 cells expressing Rluc were inoculated with 100 μL rabbit anti-VV-immunized serum (IgG fraction) before intraperitoneal injection of B5R EEV or ΔSCR EEV derived from the supernatant of infected A2780 cells. Tumor Rluc was detected on days −3 and 8, and viral Fluc was detected on days 3 and 7 after virus injection (n = 6). (B) Quantification of viral Fluc luminescence after virus injection. Solid and dashed lines represent serum (IgG)-treated and untreated cells, respectively. *p < 0.05 (two-way ANOVA). (C) Quantification of tumor Rluc luminescence before and after virus injection. Data in (B) and (C) are presented as means ± SD (n = 6). *p < 0.05 (two-way ANOVA). (D) Survival curves of mice in (A)–(C) generated by Kaplan-Meier analysis. Treatment with ΔSCR EEV + αVV Ab (IgG) prolonged survival compared to PBS + αVV Ab (p = 0.0005, log rank test) and B5R EEV + αVV Ab (p = 0.0291, log rank test).

virus sufficiently, likely due to the end of smallpox vaccination in the 1980s.

On the other hand, both anti-VV and -B5R antibodies were clearly detected in immunized monkey serum in proportion to vaccine dosage (Figures 3C and 3D). The levels of VV- and B5R-specific antibodies were measured on days 1, 3, 7, 20, and 30 after virus injection, and very high levels of antibody titers were induced after day 20 (data not shown). This was consistent with the previous finding that anti-VV antibodies are elicited in human cancer patients within 1 month after virus treatment.[55–58] Furthermore, the elicitation of anti-VV antibodies strongly decreases the viral titers in blood following repeated intravenous VV injections in cancer patients.[59] Therefore, immune resistance and oncolytic activity of VV were examined by mixing the viruses with monkey serum. High- and low-VV dose-immunized monkey sera contained anti-B5R antibody (Figure 3D) and efficiently neutralized B5R EEV (Figures 4A and 4B). On the other hand, ΔSCR EEV escaped neutralization and retained its oncolytic activity when mixed with either high- or low-dose-immunized serum (Figures 4A–4C). The former more potently neutralized EEV and IMV than did the latter, according to the recorded ELISA titers against B5R.

EEV neutralization strongly depends on anti-B5R antibody and complement, but SCR deletion enhanced EEV escape upon exposure to those neutralizers (Figures 5A and 5B). Rabbit anti-VV antibody (anti-B5R antibody) or complement alone does not neutralize EEV efficiently, but their combination markedly enhanced neutralizing activity against EEV. B5R EEV exhibited greater immune resistance than did B5R IMV (Figures 5A and 5C), although some residual antigenicity was neutralized by the antibody-complement combination. However, ΔSCR EEV showed the greatest resistance (Figures 5A and 5B), even in the presence of an antibody-complement mixture.

The enhancement of neutralization resistance was confirmed in anti-virus antibody-treated mice, in which ΔSCR EEV promoted viral replication to a greater extent than B5R EEV (Figure 6B). Furthermore, ΔSCR EEV decreased tumor burden and prolonged survival in these mice irrespective of the presence of antibody (Figures 6C and 6D), since a 100 μL volume of anti-virus antibody is equivalent to approximately 0.5% of total murine blood. These data were corroborated by the results of the *in vitro* neutralization test. This xenograft model used here is artificial, because it utilizes immunodeficient mice and a xenogeneic rabbit anti-VV antibody. This model only simulates the *in vitro* conditions in the presence of anti-virus antibodies, which cannot be used to examine the immunogenicity of SCR-deleted EEV against the actual vaccinated situation. However, rabbit antibodies (including anti-B5R antibody) exhibit activity of complement-dependent EEV neutralization (Figures 5A and 5B) similar to human antibodies.[28] SCR-deleted EEVs escaped neutralization and showed a higher therapeutic effect than did B5R EEV. Therefore, higher antibody resistance and maintenance of oncolytic effect by SCR deletion can be expected in humans with pre-existing anti-VV (anti-B5R) antibodies.

The other EEV-associated protein, A33R, has also been reported to generate EEV-neutralizing antibodies in humans and rabbits.[27] Rabbit anti-VV antibody comprises anti-A33R antibody (manufacture verified). However, SCR-deleted EEV clearly enhanced their antibody resistance through only B5R modification (Figures 5 and 6). Anti-B5R antibody is strongly elicited after vaccination in humans, compared with antibodies targeting other EEV-associated antigens (including A33R).[19] As for VV vaccination, B5R protein has a higher protective potential for lethal VV challenge than does A33R.[60] Considering this, EEV neutralization is strongly dependent on B5R-specific antibody. On the other hand, SCR-deleted EEV did not exhibit perfect resistance to antibody and complement, especially when mixed with higher concentrations (Figure 5A). This might be the result of A33R-specific antibody.

B5R-specific antibody elicitation is strongly reflected in the presence of raised anti-VV antibody titers.[19] Therefore, anti-B5R antibody is a good indicator not only for EEV protection but also for whole-VV vaccination. As for escaping neutralization by oncolytic VVs, the barrier of anti-B5R antibodies will certainly be faced, especially in patients with pre-existing antibodies. This antibody targets two major epitopes of B5R at the SCR1-SCR2 border and stalk.[26] ΔSCR harbors a deletion in the former region, which confers increased resistance against EEV-neutralizing antibody. The stalk, which is present in ΔSCR, is important not only for EEV entry[38] but also for the interaction with other EEV membrane proteins, such as A33R and A34R,[61,62] which are required for B5R incorporation into the EEV outer membrane. Deletion of both the SCR and stalk regions leads to a dramatic reduction in plaque size, comparable to that observed in whole-B5R deletion.[63] Thus, VV with partial SCR deletion (ΔSCR) shows a good balance between oncolytic activity and immune resistance. This SCR-deleted phenotype was generated in other VV strains, including western reserve (WR) and IHD-J;[18] therefore, it is adaptable for several oncolytic VVs.

In summary, our SCR-deleted virus produced highly neutralization-evasive enveloped virions that retained therapeutic efficacy irrespective of antiviral antibody. VV-specific antibodies are commonly low in patients. However, they are easily elicited after virus inoculation and strongly neutralize the virus, including its EEV form. ΔSCR-derived EEV has potential as a second candidate for treating the patients who have received one or more VV injection, due to its enhanced immune resistance against pre-existing host antibodies. ΔSCR can also serve as a vector for the delivery of therapeutic agents without interference by the host, and it can potently express loaded agents through stable viral replication. Thus, our SCR-deleted VV is a next-generation platform for oncolytic virotherapy.

MATERIALS AND METHODS

Plasmid Construction

All plasmids used for B5R recombination were generated from the pTN-B5R backbone vector and harbored the *B4R*, *B5R*, and *B6R* gene loci of LC16mO VV.[1] For whole-*B5R* deletion, the *B5R* gene in pTN-B5R was replaced with the DsRed gene derived from

pDsRed-Express-N1 (Takara Bio, Otsu, Japan). The B4R fragment was amplified from pTN-B5R using the primers 5′-CAG TCA CGA CGT TGT AAA-3′ and 5′-CAT GCG CAC CTT GAA GCG CAT GAA CTC CTT GAT GAC GTC CTC GGA GGA GGC CAT TTT TAT TTA TGA GCG TTA A-3′, and it was digested with *Not*I and *Fsp*I. The DsRed fragment was amplified from pDsRed-Express-N1 with the primers 5′-GAG TTC ATG CGC TTC AAG GT-3′ and 5′-CTC AAT TGA TTC TAG CTA TAA GTC TTT AAT CTT TTG ATA CTT GTT CGT TAT TAA TTA TTA ATT ATT TTA ACG GAT TTA TAT CTA CAG GAA CAG GTG GTG-3′, and it was digested with *Fsp*I and *Mfe*I. The digested PCR fragments were subcloned into the *Mfe*I and *Not*I sites of pTN-B5R by three-part ligation, yielding pTN-DsRed.

For SCR1–4 deletion, pTN-B5R was digested with *Not*I and *Nsp*I (B4R-B5R signal peptide) or *Nsp*I and *Sac*I (B5R stalk-B6R), and the fragments were subcloned into the *Not*I and *Sac*I sites of pTN-B5R by three-part ligation, yielding pTN-ΔSCR. The plasmids used for VGF and O1 deletion (pUC19-VGF-ST-lucGFP and pUC19-O1L-ST-BFP) were generated as previously described.[34]

Cell Culture

Human carcinoma cell lines, including pancreatic AsPC1, BxPC-3, PANC-1, and SW1990 (cultured in RPMI-1640 medium); ovarian CaOV3 (DMEM) and SKOV3 (RPMI-1640); colon Caco2 (Eagle's minimal essential medium [EMEM]), HT-29 (RPMI-1640), LoVo (Ham's F12K), and SW480 (Leibovitz's L-15); lung A549 (Ham's F12K); breast MCF-7 (EMEM) and SK-BR-3 (EMEM); hepatocellular HepG2 (EMEM); neuroblastoma SK-N-AS (DMEM) and SK-N-BE (RPMI-1640); and epithelial A431 (EMEM) and Hep2 (EMEM) cells, as well as rabbit kidney-derived RK13 cells (EMEM), were purchased from the American Type Culture Collection (Manassas, VA, USA). The A2780[64] (DMEM) and RMG-1[65] (RPMI-1640) human ovarian carcinoma cell lines were provided by Osaka University (Suita, Japan) and Saitama Medical University (Hidaka, Japan), respectively. The cells were grown in the appropriate medium (Wako, Osaka, Japan) with 10% fetal bovine serum (FBS; Corning, Oneonta, NY, USA)—except for Caco2 (20% FBS) and RK13 (5% FBS) cells—at 37°C in a humidified atmosphere of 5% CO_2.

Virus Construction

Recombinant viruses were constructed as previously described.[1] Briefly, RK13 cells were infected with LC16mO at an MOI of 0.04, then transfected with pTN-DsRed. Infected cells were harvested 2–5 days later, and recombinant LC16mO Δ-DsRed virus was selected based on DsRed expression and plaque size reduction, and it was isolated over several cycles of plaque purification. Using LC16mO Δ-DsRed as the parent virus, recombination was induced in cells transfected with pTN-ΔSCR to obtain LC16mO ΔSCR, which was selected based on the loss of DsRed fluorescence and plaque expansion.

VGF- and O1-deleted viruses (LC16mO VGF⁻/O1⁻) were generated by insertion of a gene cassette expressing luciferase-fused EGFP and BFP into the VGF and O1 gene loci, respectively. For VGF deletion, RK13 cells were infected with LC16mO and transfected with pUC19-VGF-ST-lucGFP, and LC16mO VGF⁻ was purified as described above and used to infect RK13 cells, which were simultaneously transfected with pUC19-O1L-ST-BFP. LC16mO ΔSCR VGF⁻/O1⁻ was generated by two-step recombination of the B5R gene locus with LC16mO VGF⁻/O1⁻ as the parent virus, using pTN-DsRed and pTN-ΔSCR as described above. All viruses were propagated in A549 cells and titrated in RK13 cells. Viral plaque phenotype was examined and photographed under a phase-contrast or fluorescence microscope (BZ-X700; Keyence, Osaka, Japan) during titration.

EEV and IMV Production

Progeny virus productivity was evaluated by titration. Tumor cell lines were infected with LC16mO, LC16mO Δ-DsRed, LC16mO ΔSCR, LC16mO VGF⁻/O1⁻ (B5R), or LC16mO ΔSCR VGF⁻/O1⁻ (ΔSCR) at an MOI of 0.1; 48 h later, the culture medium was collected and centrifuged at $700 \times g$ for 5 min, and the supernatant was used as the EEV. Infected cells were harvested in 1 mL Opti-MEM (Thermo Fisher Scientific, Waltham, MA, USA), and the cell-associated virions—namely, IMV—were extracted from cell lysates by freeze-thawing, sonication, and centrifugation. Both virions were titrated in RK13 cells, and viral plaques were counted 3–4 days after infection; total PFU was calculated as plaque number relative to fluid volume.

Cytotoxicity Assay

Viral cytotoxicity was determined by measuring cell viability with the (3-(4,5-dimethylthiazol-2-yl)-5-(3-carboxymethoxyphenyl)-2-(4-sulfophenyl)-2H-tetrazolium inner salt)/phenazine methosulfate assay. The oncolytic activity of EEV was evaluated based on the viability of cells treated with the culture medium of infected cells. Ovarian carcinoma cell lines were infected with LC16mO VGF⁻/O1⁻ (B5R) or LC16mO ΔSCR VGF⁻/O1⁻ (ΔSCR) at an MOI of 0, 0.001, 0.01, 0.1, or 1 at 37°C for 1 h, and virus diluents were removed and replaced with the appropriate culture medium. After 48 h, 50 μL medium (including EEV) was recovered from each culture and pipetted onto the newly seeded ovarian cancer cells, which were the same as the EEV-producing cells; 120 h later, cells were photographed under a fluorescence microscope, and viability was assessed with the CellTiter 96 Aqueous Nonradioactive Cell Proliferation Assay (Promega, Madison, WI, USA). Whole viral cytotoxicity was evaluated in cells infected with B5R or ΔSCR at the same MOI, which were also photographed and assessed for viability 120 h after infection.

Preparation of Serum Sample

Human serum samples were prepared from ovarian cancer patients at Saitama Medical University International Medical Center (Hidaka, Japan). Approval for this project was obtained from the Ethics Committee of Saitama Medical University International Medical Center (12-096) and Tottori University (2543). Immunized monkey serum was prepared for the viral toxicity test at Tsukuba Primate Research Center, National Institutes of Biomedical Innovation, Health, and

Nutrition (Tsukuba, Japan). Male *Macaca fascicularis* (2–4 years old) were intravenously injected with LC16mO VGF$^-$/O1$^-$ VV at 1×10^8 PFU (001, 002, and 003) or 1×10^7 PFU (005, 006, and 008), or they were mock infected (004, 007, and 009). The monkeys were sacrificed 30 days later, and serum was collected for analysis. The experiment was approved by the Animal Experiment Committee of National Institutes of Biomedical Innovation, Health, and Nutrition.

Analysis of Antibody Response by ELISA

Whole-virus antigen- and B5R-specific antibody titers in immunized serum were determined by ELISA as previously described.[19,66] Briefly, Immulon 2HB plates (Thermo Fisher Scientific) were coated with 5×10^6 PFU/well of whole-virus antigen, 660 ng/well of B5R, or PBS (mock). The wells were blocked at 37°C for 2 h with PBS containing 10% FBS, then washed with PBS containing 10% FBS and 0.5% Tween-20. The plates were incubated for 2 h with 4-fold serial dilutions (32×, 128×, and 512× or 4×, 16×, 64×, 256×, 1,024×, and 4,096×) of serum from human patients (221, 183, 195, 175, and 214) or monkeys immunized with high (001, 002, and 003) or low (005, 006, and 008) doses of VV or from mock-immunized monkeys (004, 007, and 009). Rabbit anti-VV serum (IgG fraction; Capricorn Scientific, Ebsdorfergrund, Germany) was used as a positive control in human serum analysis.

After washing, the wells were incubated at 37°C for 1 h with horseradish peroxidase-conjugated rabbit anti-human IgG H&L (diluted 1:4,000; SouthernBiotech, Birmingham, AL, USA), goat anti-monkey IgG H&L (diluted 1:5,000; Abcam, Cambridge, UK), or goat anti-rabbit IgG H&L (diluted 1:4,000; SouthernBiotech). A 100 μL volume of SuperSignal ELISA Femto Maximum Sensitivity Substrate (Thermo Fisher Scientific) was added to the washed wells, and optical density at 405 nm (OD_{405}) was recorded with an ARVO MX (PerkinElmer, Waltham, MA, USA). Antibody endpoint titers were defined as the reciprocal of dilutions corresponding to twice the mean OD_{405} value of PBS-coated wells.

EEV and IMV Neutralization Assays

EEV and IMV were neutralized by mixing with anti-virus IgG and complement or immunized monkey serum. EEV and IMV were recovered from the supernatant or lysate of SKOV3 cells infected with LC16mO VGF$^-$/O1$^-$ (B5R) or LC16mO ΔSCR VGF$^-$/O1$^-$ (ΔSCR) at an MOI of 0.1, as described for EEV or IMV production. In the case of rabbit IgG and complement, about 1,500–2,000 PFU EEV or 5,000–7,000 PFU IMV was mixed with 0%, 0.2%, 0.5%, or 1% rabbit anti-VV immunized serum (IgG fraction; Capricorn Scientific) and 0%, 1%, 3%, 10%, or 25% rabbit complement (Cedarlane Labs, Burlington, ON, Canada), followed by incubation at 37°C for 30 min. The virus-serum-complement mixture was used to infect newly seeded SKOV3 cells, and, after incubation at 37°C for 2 h, the mixture was removed and replaced with the appropriate culture medium. After 96 h, the cells were photographed under a fluorescence microscope, and fluorescence intensity was quantified using the Hybrid Cell Count software (Keyence), according to the manufacturer's protocol.

When RMG-1 cells were used to measure cell viability, about 1,500–5,000 PFU EEV or 6,000–7,000 PFU IMV derived from RMG-1 cells infected with B5R or ΔSCR was mixed with 0%, 0.2%, or 0.5% rabbit anti-vaccinia IgG and 0%, 1%, 3%, 10%, or 25% complement or with 0%, 0.5%, 1%, 3%, or 5% immunized monkey serum. The mixtures were incubated and used to infect newly seeded RMG-1 cells as described above. After 120 h, cells were photographed, and fluorescence and viability were quantified.

In Vivo Antibody-Treated Mouse Model

To establish an antibody-treated tumor-bearing mouse model, 6-week-old female athymic nude mice (Charles River Laboratories, Yokohama, Japan) were intraperitoneally injected with A2780 cells stably expressing Rluc (5×10^6 cells in 100 μL PBS [pH 7.4]), and they were treated 11 days later (1 day before virus injection) with 100 μL PBS or rabbit anti-VV serum (500 μg/mouse, IgG fraction; Capricorn Scientific) by intraperitoneal injection. Meanwhile, cultured A2780 cells were infected with B5R or ΔSCR at an MOI 0.05, and, 24 h later, each EEV was recovered from the culture supernatant as described above.

At 12 days after tumor transplantation, the mice were intraperitoneally injected with 500 μL PBS (mock), B5R EEV, or ΔSCR EEV (6.3×10^4 PFU or 3.5×10^5 PFU, which was determined by titration). Both antibody and EEVs were treated once. For non-invasive monitoring of tumor growth or viral replication, mice were intraperitoneally injected with 150 μL ViviRen *In Vivo* Renilla Luciferase Substrate (18.5 μg/mouse; Promega) on days 3, 8, 11, and 15 and with 200 μL VivoGlo Luciferin, *In Vivo* Grade (3 mg/mouse; Promega) on days 1, 2, 3, 5, 7, and 10 after virus injection. The mice were anesthetized with isoflurane during bioimaging; the bioluminescence of tumor Rluc or viral Fluc was detected by the injection of ViviRen and VivoGlo (Promega), respectively, and it was visualized using NightSHADE LB985 (Berthold Technologies, Bad Wildbad, Germany) and quantified according to the manufacturer's protocol. The experiment was approved by the Animal Experiment Committee of Tottori University.

Statistical Analysis

Differences in progeny virus titers and cell viability among groups were evaluated with the two-tailed unpaired t test, and *in vivo* bioluminescence was analyzed by two-way ANOVA followed by the Bonferroni test when the ANOVA showed an overall significance. Survival curves were generated with the Kaplan-Meier method and were analyzed with the log rank test. p values <0.05 were considered statistically significant. All statistical analyses were performed using Prism version (v.)5 (GraphPad, La Jolla, CA, USA).

SUPPLEMENTAL INFORMATION

Supplemental Information can be found online at https://doi.org/10.1016/j.omto.2019.05.003.

AUTHOR CONTRIBUTIONS

T.N. supervised the study. T.N., M.N., and H. Kurosaki designed the study and interpreted the results. M.N. performed most of the

experiments. M.N. and N.K. constructed recombinant vaccinia viruses. K. Horita, M.I., and H. Kono maintained the tumor cell lines. K. Hasegawa prepared human serum. T.O. and Y.Y. prepared vaccinia-immunized monkey serum. T.N. and M.N. wrote the manuscript.

REFERENCES

1. Hikichi, M., Kidokoro, M., Haraguchi, T., Iba, H., Shida, H., Tahara, H., and Nakamura, T. (2011). MicroRNA regulation of glycoprotein B5R in oncolytic vaccinia virus reduces viral pathogenicity without impairing its antitumor efficacy. Mol. Ther. 19, 1107–1115.

2. Kirn, D.H., Wang, Y., Liang, W., Contag, C.H., and Thorne, S.H. (2008). Enhancing poxvirus oncolytic effects through increased spread and immune evasion. Cancer Res. 68, 2071–2075.

3. Thirunavukarasu, P., Sathaiah, M., Gorry, M.C., O'Malley, M.E., Ravindranathan, R., Austin, F., Thorne, S.H., Guo, Z.S., and Bartlett, D.L. (2013). A rationally designed A34R mutant oncolytic poxvirus: improved efficacy in peritoneal carcinomatosis. Mol. Ther. 21, 1024–1033.

4. de Graaf, J.F., de Vor, L., Fouchier, R.A.M., and van den Hoogen, B.G. (2018). Armed oncolytic viruses: A kick-start for anti-tumor immunity. Cytokine Growth Factor Rev. 41, 28–39.

5. Thorne, S.H., Negrin, R.S., and Contag, C.H. (2006). Synergistic antitumor effects of immune cell-viral biotherapy. Science 311, 1780–1784.

6. Chang, C.L., Ma, B., Pang, X., Wu, T.C., and Hung, C.F. (2009). Treatment with cyclooxygenase-2 inhibitors enables repeated administration of vaccinia virus for control of ovarian cancer. Mol. Ther. 17, 1365–1372.

7. Guo, Z.S., Parimi, V., O'Malley, M.E., Thirunavukarasu, P., Sathaiah, M., Austin, F., and Bartlett, D.L. (2010). The combination of immunosuppression and carrier cells significantly enhances the efficacy of oncolytic poxvirus in the pre-immunized host. Gene Ther. 17, 1465–1475.

8. Ikeda, K., Ichikawa, T., Wakimoto, H., Silver, J.S., Deisboeck, T.S., Finkelstein, D., Harsh, G.R., 4th, Louis, D.N., Bartus, R.T., Hochberg, F.H., and Chiocca, E.A. (1999). Oncolytic virus therapy of multiple tumors in the brain requires suppression of innate and elicited antiviral responses. Nat. Med. 5, 881–887.

9. Roberts, K.L., and Smith, G.L. (2008). Vaccinia virus morphogenesis and dissemination. Trends Microbiol. 16, 472–479.

10. Payne, L.G. (1980). Significance of extracellular enveloped virus in the in vitro and in vivo dissemination of vaccinia. J. Gen. Virol. 50, 89–100.

11. Smith, G.L., Vanderplasschen, A., and Law, M. (2002). The formation and function of extracellular enveloped vaccinia virus. J. Gen. Virol. 83, 2915–2931.

12. Locker, J.K., Kuehn, A., Schleich, S., Rutter, G., Hohenberg, H., Wepf, R., and Griffiths, G. (2000). Entry of the two infectious forms of vaccinia virus at the plasma membrane is signaling-dependent for the IMV but not the EEV. Mol. Biol. Cell 11, 2497–2511.

13. Vanderplasschen, A., Hollinshead, M., and Smith, G.L. (1998). Intracellular and extracellular vaccinia virions enter cells by different mechanisms. J. Gen. Virol. 79, 877–887.

14. Krauss, O., Hollinshead, R., Hollinshead, M., and Smith, G.L. (2002). An investigation of incorporation of cellular antigens into vaccinia virus particles. J. Gen. Virol. 83, 2347–2359.

15. Vanderplasschen, A., Mathew, E., Hollinshead, M., Sim, R.B., and Smith, G.L. (1998). Extracellular enveloped vaccinia virus is resistant to complement because of incorporation of host complement control proteins into its envelope. Proc. Natl. Acad. Sci. USA 95, 7544–7549.

16. Ichihashi, Y. (1996). Extracellular enveloped vaccinia virus escapes neutralization. Virology 217, 478–485.

17. Blasco, R., Sisler, J.R., and Moss, B. (1993). Dissociation of progeny vaccinia virus from the cell membrane is regulated by a viral envelope glycoprotein: effect of a point mutation in the lectin homology domain of the A34R gene. J. Virol. 67, 3319–3325.

18. Bell, E., Shamim, M., Whitbeck, J.C., Sfyroera, G., Lambris, J.D., and Isaacs, S.N. (2004). Antibodies against the extracellular enveloped virus B5R protein are mainly responsible for the EEV neutralizing capacity of vaccinia immune globulin. Virology 325, 425–431.

19. Pütz, M.M., Midgley, C.M., Law, M., and Smith, G.L. (2006). Quantification of antibody responses against multiple antigens of the two infectious forms of Vaccinia virus provides a benchmark for smallpox vaccination. Nat. Med. 12, 1310–1315.

20. Doceul, V., Hollinshead, M., Breiman, A., Laval, K., and Smith, G.L. (2012). Protein B5 is required on extracellular enveloped vaccinia virus for repulsion of superinfecting virions. J. Gen. Virol. 93, 1876–1886.

21. Engelstad, M., and Smith, G.L. (1993). The vaccinia virus 42-kDa envelope protein is required for the envelopment and egress of extracellular virus and for virus virulence. Virology 194, 627–637.

22. Herrera, E., Lorenzo, M.M., Blasco, R., and Isaacs, S.N. (1998). Functional analysis of vaccinia virus B5R protein: essential role in virus envelopment is independent of a large portion of the extracellular domain. J. Virol. 72, 294–302.

23. Mathew, E., Sanderson, C.M., Hollinshead, M., and Smith, G.L. (1998). The extracellular domain of vaccinia virus protein B5R affects plaque phenotype, extracellular enveloped virus release, and intracellular actin tail formation. J. Virol. 72, 2429–2438.

24. Mathew, E.C., Sanderson, C.M., Hollinshead, R., and Smith, G.L. (2001). A mutational analysis of the vaccinia virus B5R protein. J. Gen. Virol. 82, 1199–1213.

25. Wolffe, E.J., Isaacs, S.N., and Moss, B. (1993). Deletion of the vaccinia virus B5R gene encoding a 42-kilodalton membrane glycoprotein inhibits extracellular virus envelope formation and dissemination. J. Virol. 67, 4732–4741.

26. Aldaz-Carroll, L., Whitbeck, J.C., Ponce de Leon, M., Lou, H., Hirao, L., Isaacs, S.N., Moss, B., Eisenberg, R.J., and Cohen, G.H. (2005). Epitope-mapping studies define two major neutralization sites on the vaccinia virus extracellular enveloped virus glycoprotein B5R. J. Virol. 79, 6260–6271.

27. Benhnia, M.R., Maybeno, M., Blum, D., Aguilar-Sino, R., Matho, M., Meng, X., Head, S., Felgner, P.L., Zajonc, D.M., Koriazova, L., et al. (2013). Unusual features of vaccinia virus extracellular virion form neutralization resistance revealed in human antibody responses to the smallpox vaccine. J. Virol. 87, 1569–1585.

28. Benhnia, M.R., McCausland, M.M., Laudenslager, J., Granger, S.W., Rickert, S., Koriazova, L., Tahara, T., Kubo, R.T., Kato, S., and Crotty, S. (2009). Heavily isotype-dependent protective activities of human antibodies against vaccinia virus extracellular virion antigen B5. J. Virol. 83, 12355–12367.

29. Benhnia, M.R., McCausland, M.M., Moyron, J., Laudenslager, J., Granger, S., Rickert, S., Koriazova, L., Kubo, R., Kato, S., and Crotty, S. (2009). Vaccinia virus extracellular enveloped virion neutralization in vitro and protection in vivo depend on complement. J. Virol. 83, 1201–1215.

30. Sanderson, C.M., Frischknecht, F., Way, M., Hollinshead, M., and Smith, G.L. (1998). Roles of vaccinia virus EEV-specific proteins in intracellular actin tail formation and low pH-induced cell-cell fusion. J. Gen. Virol. 79, 1415–1425.

31. Rodger, G., and Smith, G.L. (2002). Replacing the SCR domains of vaccinia virus protein B5R with EGFP causes a reduction in plaque size and actin tail formation but enveloped virions are still transported to the cell surface. J. Gen. Virol. 83, 323–332.

32. Sugimoto, M., and Yamanouchi, K. (1994). Characteristics of an attenuated vaccinia virus strain, LC16m0, and its recombinant virus vaccines. Vaccine 12, 675–681.

33. Sugimoto, M., Yasuda, A., Miki, K., Morita, M., Suzuki, K., Uchida, N., and Hashizume, S. (1985). Gene structures of low-neurovirulent vaccinia virus

LC16m0, LC16m8, and their Lister original (LO) strains. Microbiol. Immunol. *29*, 421–428.

34. Nakamura, T. (2017). Mitogen-activated protein kinase-dependent recombinant vaccinia virus (MD-RVV) and use thereof. US patent US9809803B2, filed November 20, 2014, and granted November 7, 2017.

35. Ricca, J.M., Oseledchyk, A., Walther, T., Liu, C., Mangarin, L., Merghoub, T., Wolchok, J.D., and Zamarin, D. (2018). Pre-existing immunity to oncolytic virus potentiates its immunotherapeutic efficacy. Mol. Ther. *26*, 1008–1019.

36. Lun, X.Q., Jang, J.H., Tang, N., Deng, H., Head, R., Bell, J.C., Stojdl, D.F., Nutt, C.L., Senger, D.L., Forsyth, P.A., and McCart, J.A. (2009). Efficacy of systemically administered oncolytic vaccinia virotherapy for malignant gliomas is enhanced by combination therapy with rapamycin or cyclophosphamide. Clin. Cancer Res. *15*, 2777–2788.

37. Chen, J., Gao, P., Yuan, S., Li, R., Ni, A., Chu, L., Ding, L., Sun, Y., Liu, X.Y., and Duan, Y. (2016). Oncolytic adenovirus complexes coated with lipids and calcium phosphate for cancer gene therapy. ACS Nano *10*, 11548–11560.

38. Roberts, K.L., Breiman, A., Carter, G.C., Ewles, H.A., Hollinshead, M., Law, M., and Smith, G.L. (2009). Acidic residues in the membrane-proximal stalk region of vaccinia virus protein B5 are required for glycosaminoglycan-mediated disruption of the extracellular enveloped virus outer membrane. J. Gen. Virol. *90*, 1582–1591.

39. Ward, B.M., and Moss, B. (2000). Golgi network targeting and plasma membrane internalization signals in vaccinia virus B5R envelope protein. J. Virol. *74*, 3771–3780.

40. Newsome, T.P., Scaplehorn, N., and Way, M. (2004). SRC mediates a switch from microtubule- to actin-based motility of vaccinia virus. Science *306*, 124–129.

41. Horsington, J., Lynn, H., Turnbull, L., Cheng, D., Braet, F., Diefenbach, R.J., Whitchurch, C.B., Karupiah, G., and Newsome, T.P. (2013). A36-dependent actin filament nucleation promotes release of vaccinia virus. PLoS Pathog. *9*, e1003239.

42. Pechenick Jowers, T., Featherstone, R.J., Reynolds, D.K., Brown, H.K., James, J., Prescott, A., Haga, I.R., and Beard, P.M. (2015). RAB1A promotes Vaccinia virus replication by facilitating the production of intracellular enveloped virions. Virology *475*, 66–73.

43. Harrison, K., Haga, I.R., Pechenick Jowers, T., Jasim, S., Cintrat, J.C., Gillet, D., Schmitt-John, T., Digard, P., and Beard, P.M. (2016). Vaccinia virus uses retromer-independent cellular retrograde transport pathways to facilitate the wrapping of intracellular mature virions during viral morphogenesis. J. Virol. *90*, 10120–10132.

44. Sivan, G., Weisberg, A.S., Americo, J.L., and Moss, B. (2016). Retrograde transport from early endosomes to the trans-Golgi network enables membrane wrapping and egress of vaccinia virus virions. J. Virol. *90*, 8891–8905.

45. Gao, W.N.D., Carpentier, D.C.J., Ewles, H.A., Lee, S.A., and Smith, G.L. (2017). Vaccinia virus proteins A36 and F12/E2 show strong preferences for different kinesin light chain isoforms. Traffic *18*, 505–518.

46. Hollinshead, M., Rodger, G., Van Eijl, H., Law, M., Hollinshead, R., Vaux, D.J.T., and Smith, G.L. (2001). Vaccinia virus utilizes microtubules for movement to the cell surface. J. Cell Biol. *154*, 389–402.

47. Ward, B.M., and Moss, B. (2001). Vaccinia virus intracellular movement is associated with microtubules and independent of actin tails. J. Virol. *75*, 11651–11663.

48. Kohno, T., Ichikawa, H., Totoki, Y., Yasuda, K., Hiramoto, M., Nammo, T., Sakamoto, H., Tsuta, K., Furuta, K., Shimada, Y., et al. (2012). KIF5B-RET fusions in lung adenocarcinoma. Nat. Med. *18*, 375–377.

49. Kawai, Y., Shibata, K., Sakata, J., Suzuki, S., Utsumi, F., Niimi, K., Sekiya, R., Senga, T., Kikkawa, F., and Kajiyama, H. (2018). KIF20A expression as a prognostic indicator and its possible involvement in the proliferation of ovarian clear-cell carcinoma cells. Oncol. Rep. *40*, 195–205.

50. Mittal, K., Choi, D.H., Klimov, S., Pawar, S., Kaur, R., Mitra, A.K., Gupta, M.V., Sams, R., Cantuaria, G., Rida, P.C.G., and Aneja, R. (2016). A centrosome clustering protein, KIFC1, predicts aggressive disease course in serous ovarian adenocarcinomas. J. Ovarian Res. *9*, 17.

51. Qiu, H.L., Deng, S.Z., Li, C., Tian, Z.N., Song, X.Q., Yao, G.D., and Geng, J.S. (2017). High expression of KIF14 is associated with poor prognosis in patients with epithelial ovarian cancer. Eur. Rev. Med. Pharmacol. Sci. *21*, 239–245.

52. McGrail, D.J., Khambhati, N.N., Qi, M.X., Patel, K.S., Ravikumar, N., Brandenburg, C.P., and Dawson, M.R. (2015). Alterations in ovarian cancer cell adhesion drive taxol resistance by increasing microtubule dynamics in a FAK-dependent manner. Sci. Rep. *5*, 9529.

53. Yang, H., Mao, W., Rodriguez-Aguayo, C., Mangala, L.S., Bartholomeusz, G., Iles, L.R., Jennings, N.B., Ahmed, A.A., Sood, A.K., Lopez-Berestein, G., et al. (2018). Paclitaxel sensitivity of ovarian cancer can be enhanced by knocking down pairs of kinases that regulate MAP4 phosphorylation and microtubule stability. Clin. Cancer Res. *24*, 5072–5084.

54. Breitbach, C.J., Burke, J., Jonker, D., Stephenson, J., Haas, A.R., Chow, L.Q., Nieva, J., Hwang, T.H., Moon, A., Patt, R., et al. (2011). Intravenous delivery of a multi-mechanistic cancer-targeted oncolytic poxvirus in humans. Nature *477*, 99–102.

55. Downs-Canner, S., Guo, Z.S., Ravindranathan, R., Breitbach, C.J., O'Malley, M.E., Jones, H.L., Moon, A., McCart, J.A., Shuai, Y., Zeh, H.J., and Bartlett, D.L. (2016). Phase 1 Study of Intravenous Oncolytic Poxvirus (vvDD) in Patients With Advanced Solid Cancers. Mol. Ther. *24*, 1492–1501.

56. Zeh, H.J., Downs-Canner, S., McCart, J.A., Guo, Z.S., Rao, U.N., Ramalingam, L., Thorne, S.H., Jones, H.L., Kalinski, P., Wieckowski, E., et al. (2015). First-in-man study of western reserve strain oncolytic vaccinia virus: safety, systemic spread, and antitumor activity. Mol. Ther. *23*, 202–214.

57. Lauer, U.M., Schell, M., Beil, J., Berchtold, S., Koppenhöfer, U., Glatzle, J., Königsrainer, A., Möhle, R., Nann, D., Fend, F., et al. (2018). Phase I Study of Oncolytic Vaccinia Virus GL-ONC1 in Patients with Peritoneal Carcinomatosis. Clin. Cancer Res. *24*, 4388–4398.

58. Heo, J., Reid, T., Ruo, L., Breitbach, C.J., Rose, S., Bloomston, M., Cho, M., Lim, H.Y., Chung, H.C., Kim, C.W., et al. (2013). Randomized dose-finding clinical trial of oncolytic immunotherapeutic vaccinia JX-594 in liver cancer. Nat. Med. *19*, 329–336.

59. Park, S.H., Breitbach, C.J., Lee, J., Park, J.O., Lim, H.Y., Kang, W.K., Moon, A., Mun, J.H., Sommermann, E.M., Maruri Avidal, L., et al. (2015). Phase 1b Trial of Biweekly Intravenous Pexa-Vec (JX-594), an Oncolytic and Immunotherapeutic Vaccinia Virus in Colorectal Cancer. Mol. Ther. *23*, 1532–1540.

60. Kaufman, D.R., Goudsmit, J., Holterman, L., Ewald, B.A., Denholtz, M., Devoy, C., Giri, A., Grandpre, L.E., Heraud, J.M., Franchini, G., et al. (2008). Differential antigen requirements for protection against systemic and intranasal vaccinia virus challenges in mice. J. Virol. *82*, 6829–6837.

61. Chan, W.M., and Ward, B.M. (2012). The A33-dependent incorporation of B5 into extracellular enveloped vaccinia virions is mediated through an interaction between their lumenal domains. J. Virol. *86*, 8210–8220.

62. Breiman, A., and Smith, G.L. (2010). Vaccinia virus B5 protein affects the glycosylation, localization and stability of the A34 protein. J. Gen. Virol. *91*, 1823–1827.

63. Perdiguero, B., and Blasco, R. (2006). Interaction between vaccinia virus extracellular virus envelope A33 and B5 glycoproteins. J. Virol. *80*, 8763–8777.

64. Mabuchi, S., Ohmichi, M., Nishio, Y., Hayasaka, T., Kimura, A., Ohta, T., Saito, M., Kawagoe, J., Takahashi, K., Yada-Hashimoto, N., et al. (2004). Inhibition of NFkappaB increases the efficacy of cisplatin in in vitro and in vivo ovarian cancer models. J. Biol. Chem. *279*, 23477–23485.

65. Komatsu, M., Hiyama, K., Tanimoto, K., Yunokawa, M., Otani, K., Ohtaki, M., Hiyama, E., Kigawa, J., Ohwada, M., Suzuki, M., et al. (2006). Prediction of individual response to platinum/paclitaxel combination using novel marker genes in ovarian cancers. Mol. Cancer Ther. *5*, 767–775.

66. Law, M., Pütz, M.M., and Smith, G.L. (2005). An investigation of the therapeutic value of vaccinia-immune IgG in a mouse pneumonia model. J. Gen. Virol. *86*, 991–1000.